

Effect of twin microstructure changes on the magnetization behavior and magnetic forces in Ni-Mn-Ga-based ferromagnetic shape memory alloys

Alexander LIKHACHEV^{1*}

¹ G.V. Kurdyumov Institute of Metal Physics, National Academy of Sciences of Ukraine,
Acad. Vernadsky Blvd. 36, 03680 Kyiv, Ukraine

* Corresponding author. Tel.: +380-44-4241420; fax: +380-44-4242561; e-mail: alexl@imp.kiev.ua

Received October 04, 2013; accepted December 25, 2013; available on-line August 30, 2014

The effect of twin microstructure changes on the magnetization behavior and magnetic forces in Ni-Mn-Ga-based Ferromagnetic Shape Memory Alloys (FMSMA's) is discussed on the basis of the recently developed micromagnetic theory of magnetization processes in this new class of magnetostrictive materials. A comparison between theoretical results and experiments on the superelastic behavior of Ni-Mn-Ga in an external magnetic field is also made.

Magnetic shape memory / Magnetism / Twinning / Magnetic free energy / Magnetic driving force / Superelastic behavior

Introduction

Ni-Mn-Ga-based Ferromagnetic Shape Memory Alloys (FMSMA's) have been actively investigated during the past years due to their ability to show extremely large magnetic field induced deformation effects that are about 30-50 times larger, compared to the best known ordinary magnetoelastic magnetostrictive materials. The first ideas on FMSMA's were proposed by K. Ullakko in 1996 [1], who defined them as a new class of magnetostrictive materials where the large field induced strain effect is based on a twinning mechanism. Later, this idea was confirmed experimentally and large strain effects, shown in Fig. 1, were discovered in two different nonstoichiometric ferromagnetic martensitic phases of Ni-Mn-Ga (first, 6% in 5M(Ni₄₈Mn₃₀Ga₂₂) [2], and then 10% in 7M(Ni₄₉Mn₃₀Ga₂₁) [3]). The initial idea has been developed and improved by other researchers [4-9]. Many new interesting magnetomechanical effects have also been discovered experimentally and understood theoretically in Ni-Mn-Ga-based FMSMA's [10-19].

It has been also found that the strain mechanism in FMSMA's is based on twin boundary motion (indicated by white arrows) and the resulting redistribution between the two twin related variants A and B of the martensitic phase, having their easy magnetization axes perpendicular to each other, as shown in Fig. 2.

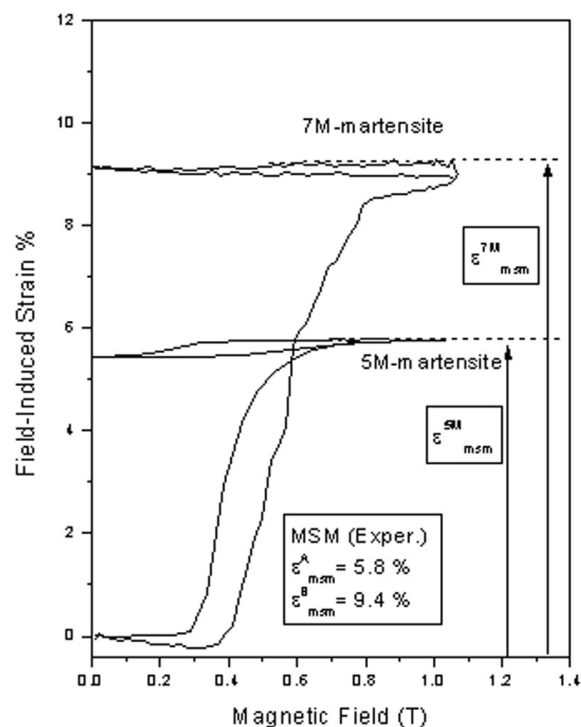


Fig. 1 Results of field-induced strain measurements in 5M and 7M Ni-Mn-Ga martensites.

Hence, the twinning process is developed in such a way that the volume fraction of the variant A, $x_A(h)$ (the magnetic domain walls of which are parallel to the direction of the magnetic field) increases. At the same time, the volume fraction of the variant B, $x_B(h)$ (where the magnetic field is perpendicular to the domain walls), decreases. As a result, the strain component along the applied magnetic field $\varepsilon(h)$ changes proportionally to the volume fraction of the variant A.

$$\varepsilon(h) = \varepsilon_0 \cdot x_A(h), \quad (1)$$

where ε_0 is a crystallographic constant characterizing the maximal strain that can be provided by the twinning mechanism. It can be measured in mechanical testing experiments or estimated from the crystal lattice parameters. In both cases it gives 6% for the 5M and 10% for the 7M phases of the Ni–Mn–Ga alloys.

There is also a general agreement that the twinning process in FMSMA's is driven by magnetostrictive forces that can be defined on a general thermodynamic basis [8-10] as follows:

$$\sigma_{mag}(h, x_A) = - \left[\frac{\partial}{\partial \varepsilon} g_{mag}(h, x_A) \right]_h, \text{ where } \varepsilon = \varepsilon_0 x_A. \quad (2)$$

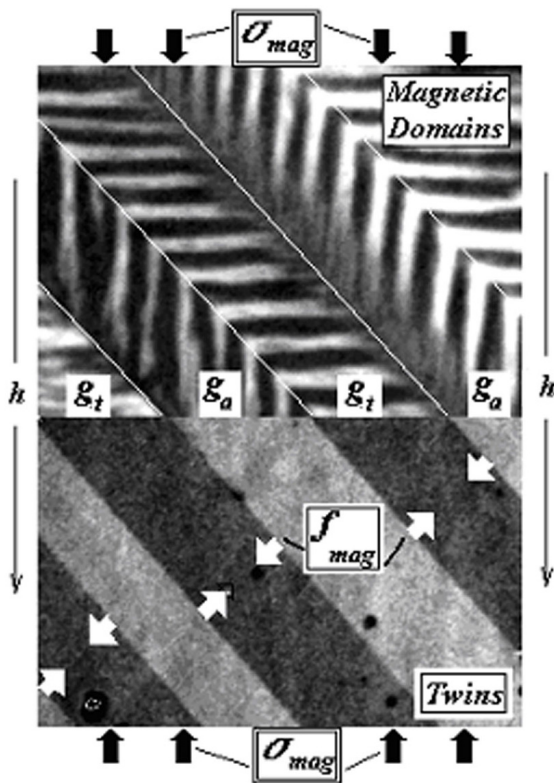


Fig. 2 Multiple twin and internal magnetic domain microstructure observed in a 5M Ni–Mn–Ga martensite ferromagnetic shape memory alloy.

Here, $g_{mag}(h, x_A)$ is the magnetic free energy of the FMSMA system and $\sigma_{mag}(h, x_A)$ represents the uniaxial magnetostrictive force (also called magnetic stress) acting along the applied external field. The macroscopic strain effect $\varepsilon(h)$ can be found as a solution of the following basic strain-stress relationships:

$$\sigma_{mag}(h, x_A) = \sigma_0(\varepsilon), \text{ with } \varepsilon = \varepsilon_0 x_A, \quad (3)$$

where $\sigma_0(\varepsilon)$ represents a zero-field stress-strain relationship for an ordinary mechanical twinning process. The magnetostrictive force plays the role of an external mechanical load, generally dependent on the magnetic field and the volume fraction of the twin variants.

The magnetic force as a function of the magnetic field and volume fraction can be measured experimentally in two different ways: by producing direct magnetization measurements for different constant volume fractions of twin variants, or by performing mechanical testing experiments in different constant magnetic fields applied perpendicular to the external load direction [11,12].

Understanding the field and the volume fraction dependence of the magnetic free energy and the magnetostrictive forces is a complex theoretical problem. Its solution is strictly dependent on our understanding of the details of the magnetization processes in FMSMA's consisting of a multiple twin band system containing a large number of magnetic domains.

The aim of the present paper was to investigate the effect of the twin and domain microstructure on the magnetic free energy and the magnetostrictive forces in the 5M martensitic phase of Ni–Mn–Ga, and discuss these results on the basis of experiments and a recently developed micromagnetic theory [13].

Experimental

In this section we briefly discuss the results of mechanical testing experiments performed on the 5M martensitic phase of Ni–Mn–Ga under a constant magnetic field, applied perpendicular to the compression direction. These experiments are interesting, not only from the point of view of a new effect of rubber-like (superelastic) behavior discovered in the 5M and 7M martensitic phases of Ni–Mn–Ga [11], but also because the magnetic driving forces and magnetic free energy of FMSMA's can be practically measured from these mechanical testing experiments [12]. This fact directly follows from the basic stress-strain relationship represented below:

$$\sigma - \sigma_{mag}(h, \varepsilon) = \sigma_0(\varepsilon), \text{ with } \varepsilon = \varepsilon_0 x_B, \quad (4)$$

where σ is the external uniaxial compression stress and ε denotes the strain component along the load direction. Accordingly, the magnetostrictive force can be found as the difference between the twinning stress measured in a constant magnetic field and the zero field twinning stress $\sigma_0(\varepsilon)$.

The samples of the 5M martensitic phase investigated experimentally were first subjected to all the necessary preparation procedures, including heat treatment, orientation with respect to the crystallographic axes, cutting, polishing and electropolishing. Then all of them were mechanically transformed from the usual multi-variant mixture of martensite variants into a standard single-variant state. Having a 5M type of martensite crystal structure, it has high martensitic transformation and Curie temperatures ($M_s = 42^\circ\text{C}$; $T_C = 103^\circ\text{C}$), high magnetic anisotropy and low 1 MPa zero field twinning stresses.

Mechanical testing experiments were performed using a standard Lloyd Instruments machine, additionally equipped with an electromagnet. The magnetic fields were changed in 0.1 T steps, starting from zero and finishing at 1 T. The obtained results are shown in Fig. 3. It follows from Fig. 3 that an increase of the magnetic field monotonically shifts the stress-strain curves up to higher stress values and changes their shape.

In accordance with Eq. 4, the magnetostrictive force was found as the difference between the twinning stress measured in a constant magnetic field and the zero field twinning stress curves $\sigma_0(\varepsilon)$ within the strain range 1-5%.

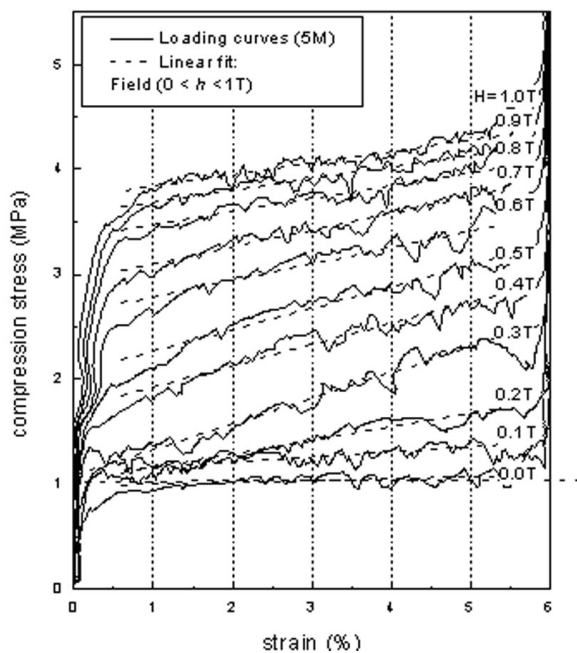


Fig. 3 Effect of magnetic field on the stress-strain relationship in 5M Ni-Mn-Ga martensite.

The corresponding values are shown in Fig. 4. It can be seen that the magnetic force is strongly dependent both on the magnetic field and on the strain (volume fraction). Within the strain range 1~5%, the magnetic force shows linear dependence on the volume fraction and can be represented as the sum of two contributions:

$$\sigma_{mag}(h, x_A) = \sigma_{mag}^0(h) + \left(x_A - \frac{1}{2}\right) \sigma_{mag}^{int}(h). \quad (5)$$

Both these contributions are plotted in Fig. 5.

In the next section we will discuss the behavior of the magnetostrictive forces on the basis of a recently developed micromagnetic theory [13].

Results

The picture presented in Fig. 2 reveals a complex multi-scale microstructure in the 5M martensitic phase of Ni-Mn-Ga. It shows a two-variant martensite microstructure consisting of multiple twin bands separated by twin boundaries. There is also a fine magnetic domain microstructure within each twin band with 180° domain walls parallel to the local easy magnetization axes of the twin variants, and approximately perpendicular to each other.

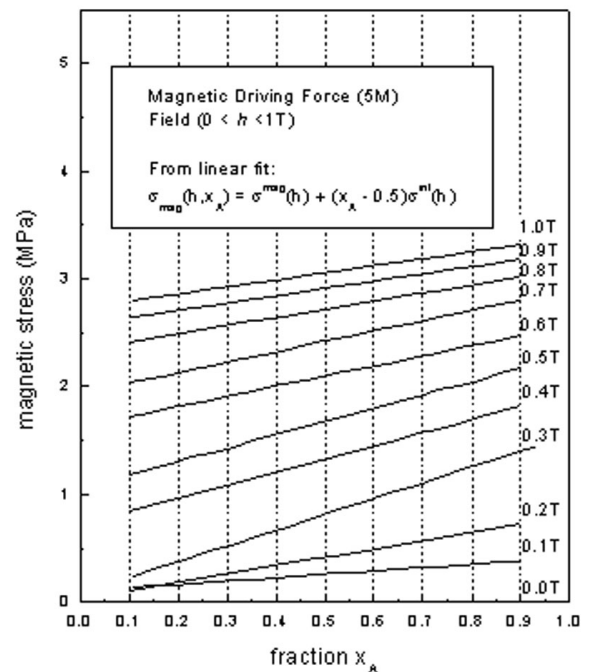


Fig. 4 Volume fraction dependence of the magnetostrictive force as found from mechanical testing experiments in different constant magnetic fields for 5M Ni-Mn-Ga martensite.

Following the general micromagnetic theory proposed in [13], the magnetic free energy of such a system magnetized in an external magnetic field h consists of Zeeman and magnetic anisotropy energies and a magnetostatic (demagnetizing) energy contribution. It can be represented as the sum of two terms. The first of them is linear with respect to the volume fractions x_A and x_B and describes a system consisting of two non-interacting twin variants:

$$g^0 = x_A \left(K_u \left(\frac{m_{A\perp}}{M_s} \right) - h m_A + m_A \frac{\hat{D}}{2} m_A \right) + x_B \left(K_u \left(\frac{m_{B\perp}}{M_s} \right) - h m_B + m_B \frac{\hat{D}}{2} m_B \right). \quad (6)$$

The second term is proportional to their product and therefore represents the magnetostatic interaction (coupling) energy between the two different twin variants:

$$g_{\text{int}} = \frac{1}{2} x_A x_B (m_A - m_B) 4\pi (\hat{S} - \hat{D}) (m_A - m_B). \quad (7)$$

The terms in parentheses in Eq. 6 represent the local magnetic free energies associated with the A and B variants, respectively; m_A and m_B are their local magnetization, averaged over the local magnetic domain microstructure. The first term in the parentheses is the magnetic anisotropy energy, where K_u and M_s are the magnetic anisotropy constant and the saturation magnetization value of the MSM material; $m_{A\perp}$ and $m_{B\perp}$ are projections of the magnetization on the plane perpendicular to the local easy magnetization direction of the martensite variants. The second and third terms represent the Zeeman and magnetostatic energies, respectively, where \hat{D} is the so-called demagnetizing matrix, which only depends on the macroscopic shape of the ferromagnetic sample. The other matrix introduced in Eq. 7, $\hat{S} = n \otimes n$, characterizes the demagnetizing effect of the flat twin boundaries and n means their unit normal direction vector. The magnetic free energy represented by Eqs. 6 and 7 should finally be minimized to find the local magnetizations, $m_A(h, x_A)$, $m_B(h, x_B)$, and also the total magnetic free energy $g_{\text{mag}}(h, x_A) = g^0(h, x_A) + g_{\text{int}}(h, x_A)$ as a function of the external magnetic field and volume fraction. Finally, the magnetic driving force $\sigma_{\text{mag}}(h, x_A)$ can be found using Eq. 2. Unfortunately, in the presence of magnetostatic coupling between the twin variants, the minimizing procedure given by Eq. 7 can only be produced numerically. Nevertheless, to see analytically the effects produced by the coupling energy, we can use the perturbation theory and obtain both the total magnetic free energy and the magnetic driving forces. First, we neglect the coupling term (Eq. 5) and minimize a zero-order perturbation theory model (Eq. 6), which is known and widely discussed

in the literature [8-10]. Within the zero-order approach, the local magnetizations are parallel to the external field $m_A(h) = M_s(h/h^A)$, $m_B(h) = M_s(h/h^B)$ and increase linearly to their saturation. Here, the local saturation fields are: $h^A = 4\pi D M_s$, $h^B = h^A + 2K_u/M_s$, where D is the component of the demagnetizing matrix along the field direction. The magnetic driving force according to Eq. 2 will consist of two parts: a zero-order contribution $\sigma_{\text{mag}}^0(h)$ obtained from Eq. 6 and a first-order perturbation term $\sigma_{\text{int}}(h, x_A)$ obtained from Eq. 7:

$$\sigma_{\text{mag}}^0(h) = \epsilon_0^{-1} \int_0^h (m_A(h) - m_B(h)) dh, \quad (8)$$

$$\sigma_{\text{int}}(h, x_A) = (4\pi \epsilon_0^{-1}) \left(x_A - \frac{1}{2} \right) (S - D) (m_A(h) - m_B(h))^2. \quad (9)$$

Here, $S = (n e_h)^2 = 0.5$ and n and e_h are unit vectors parallel to the twin boundary normal and the magnetic field direction.

Discussion

As follows from Eq. 6, the zero-order magnetic driving force is not dependent on the volume fractions occupied by the different twin variants. Fig. 5 shows

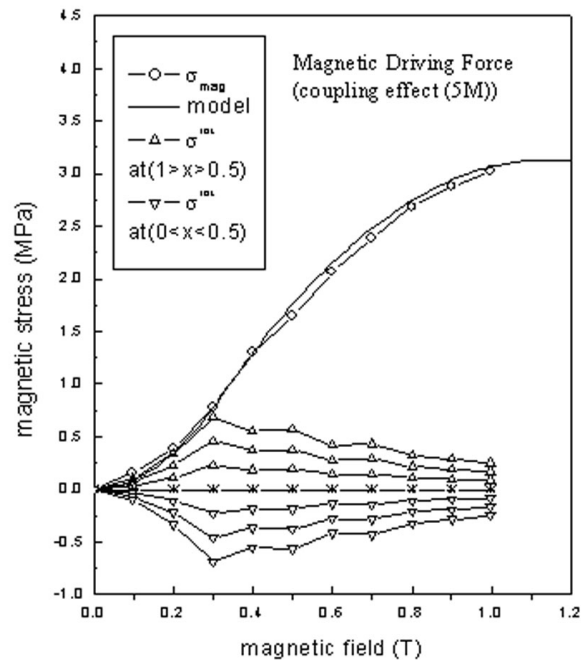


Fig. 5 Field dependence of the magnetostrictive force for different volume fractions as found from mechanical testing experiments in different constant magnetic fields for 5M Ni–Mn–Ga martensite.

that the fraction independent contribution of the magnetostrictive force measured in the mechanical testing experiments is in good agreement with the zero-order theoretical calculation made on the basis of Eq. 6. For the calculations we used the following material parameters: magnetic anisotropy constant $K_u = 1.82 \cdot 10^5 \text{ J/m}^3$; saturation magnetization $M_s = 458 \text{ G}$; demagnetizing factor for a particular sample $D = 0.58$.

The second contribution, which strongly depends both on the magnetic field and the volume fraction, can only be explained on the basis of the general micromagnetic theory according to Eq. 9. This term, caused by the magnetostatic coupling energy in Eq. 7, strongly depends on the volume fractions. It can be proven that this contribution initially increases with increasing magnetic field and reaches its maximal value at $h = h^A = 4\pi DM_s$. Then, it decreases and becomes zero at $h = h^B = h^A + 2K_u/M_s$ when the MSM material becomes fully saturated. It is interesting that both the micromagnetic theory and the experiment predict that the coupling effect may completely disappear in two cases. It may happen if the volume fractions of the twin variants are equal and if the demagnetizing effects of the external surface D and the twin interfaces S are equal to each other. We expect that future numerical solutions will improve the simple results obtained within the framework of the perturbation theory and will give us more accurate understanding of many interesting magnetomechanical effects of FMSMA's.

References

- [1] K. Ullakko, *J. Mater. Eng. Perform.* 5 (1996) 405-409.
- [2] S.J. Murrey, M. Marioni, S.M. Allen, R.C. O'Handley, *Appl. Phys. Lett.* 77 (2000) 886-888.
- [3] A. Sozinov, A.A. Likhachev, N. Lanska, K. Ullakko, *Appl. Phys. Lett.* 80 (2002) 1746-1748.
- [4] K. Ullakko, J.K. Huang, C. Kantner, R.C. O'Handley, V.V. Kokorin, *Appl. Phys. Lett.* 69 (1996) 1966-1968.
- [5] K. Ullakko, J.K. Huang, V.V. Kokorin, R.C. O'Handley, *Scripta Mater.* 36 (1997) 1133-1138.
- [6] R.C. O'Handley, *J. Appl. Phys.* 83 (1998) 3263-3270.
- [7] R.D. James, R. Tickle, M. Wuttig, *Mater. Sci. Eng. A* 273-275 (1999) 320-325.
- [8] A.A. Likhachev, K. Ullakko, *Eur. Phys. J. B* 2 (1999) 1-9.
- [9] A.A. Likhachev, K. Ullakko, *Phys. Lett. A* 275 (2000) 142-151.
- [10] A.A. Likhachev, K. Ullakko, *J. Phys. IV* 11 (2001) Pr8-293-Pr8-298.
- [11] A.A. Likhachev, A. Sozinov, K. Ullakko, *Proc. SPIE* 5387 (2004) 128-136.
- [12] A.A. Likhachev, A. Sozinov, K. Ullakko, *Mater. Sci. Eng. A* 378(1-2) (2004) 513-518.
- [13] A.A. Likhachev, A. Sozinov, K. Ullakko, *Mech. Mater.* 38(5-6) (2006) 551-563.
- [14] A.A. Likhachev, *Mater. Sci. Forum* 738-739 (2013) 405-410.
- [15] O. Heczko, *J. Magn. Magn. Mater.* 290-291 (2005) 787-794.
- [16] L. Straka, O. Heczko, *J. Magn. Magn. Mater.* 290-291 (2005) 829-831.
- [17] U. Gaitzsch, H. Klauß, S. Roth, L. Schultz, *J. Magn. Magn. Mater.* 324 (2012) 430-433.
- [18] Z. Li, Y. Zhang, C. Esling, X. Zhao, L. Zuo, *Acta Mater.* 59 (2011) 3390-3397.
- [19] O. Heczko, J. Kopeček, L. Straka, H. Seiner, *Mater. Res. Bull.* 48 (2013) 5105-5109.